On Performance of Analog Least Mean Square Loop for Self-Interference Cancellation in In-band Full-Duplex OFDM Systems

Anh Tuyen Le
University of Technology Sydney
NSW, Australia
Email: anhtuyen.le@student.uts.edu.au

Le Chung Tran
University of Wollongong
NSW, Australia
Email: lctran@uow.edu.au

Xiaojing Huang
University of Technology Sydney
NSW, Australia
Email: Xiaojing.Huang@uts.edu.au

***Abstract*—This paper evaluates the performance of analog least mean square (ALMS) loop employed to cancel self-interference in orthogonal frequency division multiplexing (OFDM) in-band full-duplex systems. Cyclostationary analysis is applied to investigate the behavior of the ALMS filter. It is revealed that the performance of the ALMS filter for OFDM system primarily depends on windowing function rather than pulse shaping as in single carrier system. It is also noticed that the ALMS loop in OFDM systems gives much higher level of sel-interference suppression because OFDM signals lead to reduce the error of the interference channel modelling with the adaptive filter. Simulation is then conducted to verify the theoretical findings.**

***Index Terms*—Full-duplex, self-interference cancellation, ALMS loop, OFDM.**

I. Introduction

It is estimated that the number of mobile users will be 70 percent of global population in 2020 [1]. This huge demand urges researchers to find out a better use of the frequency resource. In-band full-duplex radio is a promising solution for this problem because it can provide double spectral efficiency by allowing terminals to transmit and receive at the same time on the same frequency. However, it is very challenging to realize this scheme due to self-interference (SI) caused by the transmitter to its receiver. Because of the in-band full-duplex operation, it is impossible to remove this SI by just using a traditional filter. Therefore, canceling SI is the most important task for enabling full-duplex radios.

Many different approaches have been proposed in literature to tackle the problem of SI. They can be categorized into three groups including propagation domain, analog (Radio Frequency, RF) domain, and digital domain [2]. It was also proved in [2] that cancellation in analog domain is the most effective one because propagation approaches are limited by the size of devices, while digital domain cancellation cannot suppress interference more than the effective dynamic range of the analog to digital converter. The idea of analog cancellation is to produce a signal that mimics the SI in order to subtract it at the input of the receiver. It was also suggested that the cancellation signal should be captured at the output of the power amplifier (PA) to include the non-linearity components of the transmitter [3]–[5]. The amplitude and phase of this signal is then modified by a mechanism in the cancellation circuit. This mechanism can be a single tap [6], [7] or multi-tap [3], [5], [8] analog filter. Kolodziej et. al. [5] indicated that the single-tap mechanism is not effective with wide band applications and cannot cancel the reflected path components. The multi-tap mechanism, however, suffers the difficulty of calculating weight coefficients to adaptively adjust the phase and amplitude of the cancellation signal. Specifically, an additional digital algorithm is required [3], [5] or a down-conversion is applied to convert RF signals to baseband for adaptive control [9], [10]. Obviously, these approaches not only suffer problems of complexity and power consumption, but, more importantly, also introduce more noise and interference due to the additional local oscillators. To avoid these problems, a novel approach was proposed by utilising an analog least mean square (ALMS) loop which is a multi-tap structure with a low-pass filter (LPF) to replace the ideal integrator in the original ALMS loop [4]. However, the analysis was only conducted for a single carrier system.

This paper aims to investigate the behavior of the ALMS loop for multi-carrier system such as an OFDM system by applying the same cyclostationary analysis and stationary analysis. The cyclosationary analysis shows that the performance of the ALMS loop in an OFDM in-band full-duplex system is affected by the windowing function applied rather than the pulse shaping function as in single carrier counterpart. The convergence speed of the ALMS loop is determined by the length of OFDM symbol period such that the longer the OFDM symbol period, the slower the convergence speed. It is also noticed that the ALMS loop applied to OFDM signal is less sensitive to the tap delay used in the adaptive filter for self-interference cancellation.

The rest of this paper is organised as follows. In section II, the OFDM system model and the ALMS loop filter are described. In Section III, we apply cyclosationary analysis to evaluate the behavior of the ALMS loop. In Section IV,

simulations are conducted with two different scenarios of the self-interference channel to verify the theoretical analysis. Finally, conclusions are drawn in Section V.

II. System Description

A. OFDM System Model

In an OFDM system, the transmitted signal $x(t)$ is defined as

$$x(t) = Re\{X(t)e^{j2\pi f_c t}\} \tag{1}$$

where $X(t)$ is the complex envelope of the OFDM signal with a cyclic prefix and f_c is the carrier frequency. $X(t)$ is represented by

$$X(t) = \sum_{n=-\infty}^{\infty} \sum_{m=-\infty}^{\infty} \sum_{k=-N_{st}/2, k\neq 0}^{N_{st}/2} a_{k,m} e^{j2\pi \frac{k}{N}(n - m\frac{T}{T_s})} \times w(n - m\frac{T}{T_s}) p(t - nT_s) \tag{2}$$

where k is the k-th sub-carrier; m is the m-th OFDM symbol; n is the sample index; t is continuous time; T_s is the sampling period of the baseband signal; T is the OFDM symbol period; N_{st} is the total number of data subcarriers; N is the number of samples in one OFDM symbol excluding cyclic prefix; $w(n)$ is the windowing function; and $p(t)$ is the pulse shaping function.The root mean squared amplitude of transmitted signal is defined as $V_X = \sqrt{\frac{1}{T}\int_0^T E\{|X(t)|^2\}dt}$, where $E\{.\}$ stands for expectation. The load is normalized to 1Ω so that the average power of $X(t)$ is V_X^2. The complex data symbols $a_{k,m}$ are assumed to be independent to each other such that the ensemble expectation

$$E\{a^*_{k,m} a_{k',m'}\} = \begin{cases} 1, & \text{for } k = k', m = m' \\ 0, & \text{for } k \neq k', m \neq m'. \end{cases} \tag{3}$$

B. ALMS Loop

The architecture of the ALMS loop proposed in [4] is shown in Fig. 1. This is a multi-tap mechanism in which each tap has a fixed delay T_d. The cancellation circuit works as follows. The transmitted signal $x(t)$ is passed into the ALMS filter which includes L-stage taps. At the l-th tap, the transmitted signal $x(t)$ is delayed by $(l-1)T_d$ before multiplied by the amplified residual signal $d(t)$. This product is filtered by a LPF to generate weight coefficient $w_l(t)$ which will modify another version of the delayed signal $x(t)$. The outputs of all the taps are added together to obtain the cancellation signal $y(t)$. This cancellation signal is then used to subtract the SI $z(t)$ from the received signal $r(t)$. The involvement of the residual signal $d(t)$ to adaptively change weights coefficients forms a closed loop of the ALMS filter. As expressed in [4], the weighting coefficients $w_l(t)$ of l-th tap can be derived from

$$w_l(t) = \frac{2\mu\alpha}{K_1 K_2} \int_0^t e^{-(\alpha-\tau)}[r(\tau) - y(\tau)] .X(\tau - lT_d) e^{j2\pi f_c(\tau - lT_d)} d\tau \tag{4}$$

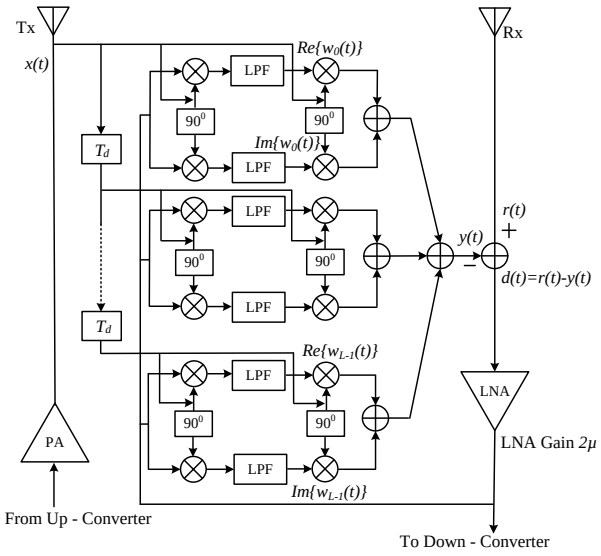

Fig. 1. The ALMS loop structure

where K_1 and K_2 are the dimensional constants of the first and second multipliers in the loop; $\alpha = \frac{1}{RC}$ is the parameter of the LPF; and 2μ is the gain of the low noise amplifier (LNA).

III. Cyclostationary analysis

Cyclostationary analysis is applied to evaluate the performance of the ALMS loop under the impact of several factors including the properties of the transmitted signal, loop gain, and the parameter of the LPF. This analysis is important to derive the lower bound of the ALMS loop.

A. Auto-Correlation Function

The auto-correlation function of an OFDM signal is defined as $\Phi_{XX}(t,\tau) = E\{X^*(t)X(t-\tau)\}$. Let $l = n - mT/T_s$ in (3) and define $g(t,\tau) = \sum_{m=-\infty}^{\infty} p^*(t - mT)p(t - mT - \tau)$. Using the property expressed in (3), the auto-correlation function can be rewritten as

$$\Phi_{XX}(t,\tau) = \sum_{l=-\infty}^{\infty} \sum_{l'=-\infty}^{\infty} \sum_{k=-N_{st}/2, k\neq 0}^{N_{st}/2} e^{-j2\pi \frac{k}{N}(l'-l)} \times w(l)w(l')g(t - lT_s, (l' - l)T_s + \tau). \tag{5}$$

With a Raised Cosine pulse shaping function $p(t)$, $g(t)$ is shown in Fig. 2. We can see that $g(t,\tau) \approx 0$ when τ is any integer multiple of T_s. Therefore, the auto-correlation function at $\tau = 0$ can be approximate as $\Phi_{XX}(t,0) = N_{st}\sum_{l=-\infty}^{\infty} w^2(l)g(t - lT_s, 0)$. For simplicity, we can further approximate the convolution of $w^2(l)$ with $g(t,0)$ as a continuous function $w^2(t)$ such that $\Phi_{XX}(t,0) \approx N_{st}w^2(t)$.

B. Solution for Weight Error Function

The interference channel is modeled as a multi-tap filter so that the equivalent baseband $Z(t)$ of the SI can be expressed

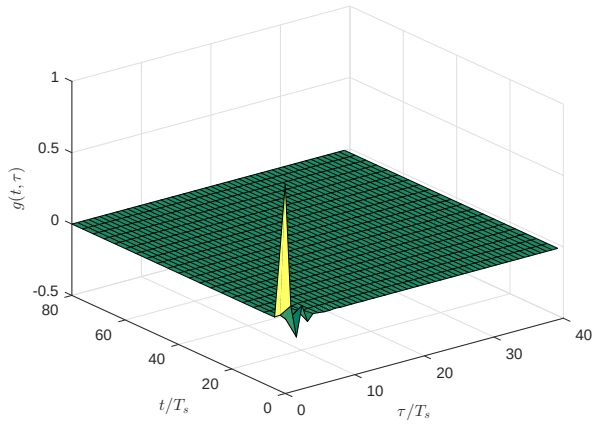

Fig. 2. $g(t,\tau)$

as $Z(t) = \sum_{l=0}^{L-1} h_l^* X(t - lT_s)$ where L is the number of taps, and tap delay is equal to the sampling rate T_s for simplicity. The performance of ALMS loop therefore can be represented by the error $u_l(t)$ between the l-th tap coefficient of interference channel model and the corresponding weight of the adaptive filter. The expected value of $u_l(t)$ is derived in [4] as $\bar{u}_l(t) = h_l - \frac{\mu\alpha}{K_1 K_2} \int_0^t \mathrm{e}^{-\alpha(t-\tau)} \bar{u}_l(\tau) \tilde{\Phi}_{XX}(\tau, 0) \mathrm{d}\tau$ where $\tilde{\Phi}_{XX}(\tau,0) = \frac{1}{V_X^2}\Phi(t,0)$ is the normalized autocorrelation function. Solving this equation, we get the final expression of $\bar{u}_l(t)$ as

$$\bar{u}_l(t) = h_l[\frac{1+\mu A^2 e^{-\alpha(1+\mu A^2)t}}{1+\mu A^2}] e^{-\alpha\mu A^2 \int_0^t (\tilde{\Phi}_{XX}(\tau,0)-1)d\tau} \tag{6}$$

where $A = V_X/\sqrt{K_1 K_2}$. Applying the windowing function recommended in IEEE802.11a

$$w(t) = \begin{cases} sin^2(\frac{\pi}{2}(\frac{t}{T_1})) & 0 \le t < T_1 \\ 1 & T_1 \le t < T_2 \\ sin^2(\frac{\pi}{2}(\frac{T-t}{T_1})) & T_2 \le m < T \end{cases} \tag{7}$$

where $T_1 = \beta T/(1+\beta)$ and $T_2 = T/(1+\beta)$ with β as the roll-off factor of the windowing function, we have

$$\bar{u}_l(t) = h_l \frac{1+\mu A^2 e^{-\alpha(1+\mu A^2)t}}{1+\mu A^2} e^{-\alpha\mu A^2 q(t)} \tag{8}$$

with $q(t)$ in period $[0,T]$ derived as

$$q(t) = \begin{cases} \frac{5(\beta-1)}{2(4-\beta)}t - \frac{2\beta T}{(4-\beta)\pi} sin(\frac{\pi t}{T_1}) + \\ \frac{\beta T}{4\pi(4-\beta)} sin(\frac{2\pi t}{T_1}) & 0 \le t < T_1 \\ \frac{5\beta}{4-\beta}(t - T/2) & T_1 \le t < T_2 \\ \frac{5(\beta-1)}{2(4-\beta)}(t-T) + \frac{2\beta T}{(4-\beta)\pi} sin(\frac{\pi(T-t)}{T_1}) - \\ \frac{\beta T}{4\pi(4-\beta)} sin(\frac{2\pi(T-t)}{T_1}) & T_2 \le t < T. \end{cases} \tag{9}$$

Since $q(t)$ is a periodic function with a period of T, the error function $\bar{u}_l(t)$ has cyclosationary property, i.e., it does not converge to a stable value but varies accordingly. The normalized $\bar{u}_l(t)$ and its variation with the error without cyclostationary behavior $\tilde{u}_l(t)$ are presented in Fig.3(a) and Fig.3(b) respectively.

C. Discussion

1) When applied to a multi-carrier system, the ALMS loop behaves similarly as in single carrier counterpart. One difference is that the weight error function $\bar{u}_l(t)$ and $\tilde{u}_l(t)$ are both periodical of OFDM symbol period T and respectively converge to $h_l \frac{1}{1+\mu A^2} e^{-\mu A^2 \alpha q(t)}$ and $h_l \frac{1}{1+\mu A^2}(e^{-\mu A^2 \alpha q(t)} - 1)$ when $t \to \infty$. The convergence speed is driven by the loop gain μA^2 and the LPF parameter α. However, with the same parameters of the ALMS loop, since one OFDM symbol includes N data samples, the convergence speed of the weighting error function in OFDM system is slower than that in single carrier system.
2) The residual interference power and interference suppression ratio (ISR) can be calculated as in [4] $P_{RI} = \frac{1}{1+\mu A^2}\frac{A^2}{2}\sum_{l=0}^{L-1}|h_l|^2$ and $ISR = \frac{P_{RI}}{P_I} = \frac{1}{(1+\mu A^2)^2}$ respectively.
3) The irreducible interference power is calculated by

$$\begin{aligned} P_{II} &= P_I \frac{1}{T}\int_0^T [\frac{1}{1+\mu A^2}(e^{-\alpha\mu A^2 q(t)} - 1)]^2 dt \\ &\approx P_I \frac{1}{T}\int_0^T [\alpha q(t)]^2 dt. \end{aligned} \tag{10}$$

Therefore, irreducible ISR lower bound is:

$$\begin{aligned} ISRLB = &\frac{\alpha^2 T^2 \beta^2}{(4-\beta)^2(1+\beta)^2}\{\frac{25}{12}(1-\beta)^2 \\ &+ \frac{5\beta}{16\pi^2}(81 - 55\beta)\}. \end{aligned} \tag{11}$$

From (11), we can see that the ISRLB of OFDM system is determined by the low-pass filter constant α and the roll-off factor of windowing function. This relationship is presented in Fig.4.

Fig.4 shows that windowing function plays an important role in the performance of ALMS filter. The ISRLB becomes smaller if the windowing function has closer form of the rectangular one.

From the ISRLB expression, we can determine the LPF parameter in order that the ISRLB is much smaller than ISR. In this case, stationary analysis can be applied to evaluate the behavior of the ALMS loop. Under this macro-scale analysis, the weight error function and interference residual power are solved with non-ideal signal autocorrelation, fractionally-spaced taps ALMS filter and general interference channel. Since the transmitted signal is treated as a stationary process, both ensemble expectation and time average is applied for the auto-correlation function of OFDM signal. It means that the

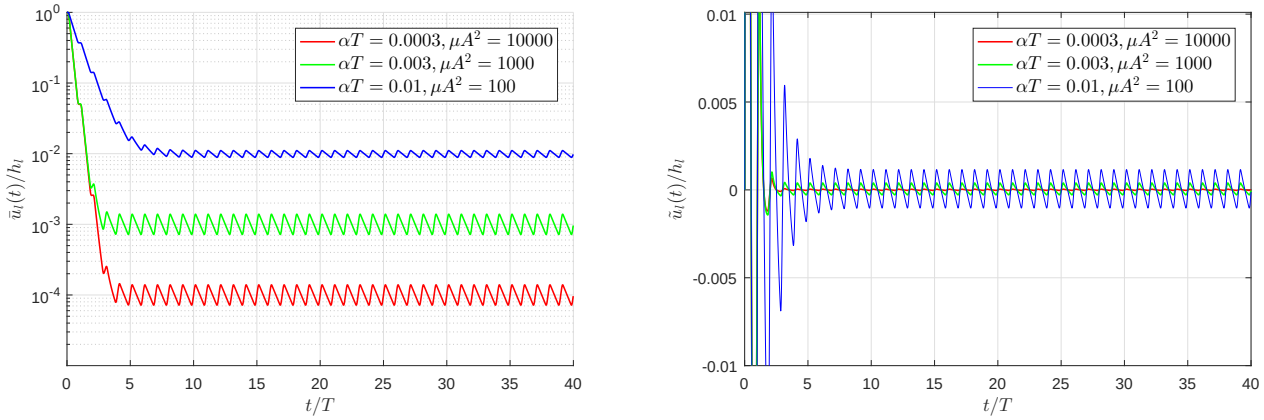

(a) (b)

Fig. 3. (a) Normalized weight error; and (b) Normalized weight error variations

solutions for the time and ensemble averaged weight function $\bar{\bar{w}}(t)$ and the residual interference power P_{RI} are not different from those of single carrier case. Therefore, we can apply the results derived in [4] for this case. Specifically, the matrix of weight function $\bar{\bar{\mathbf{w}}}(t) = [\bar{\bar{w}}_0(t)\ \bar{\bar{w}}_1(t)..\ \bar{\bar{w}}_{L-1}(t)]^T$ is found as

$$\begin{aligned}\bar{\bar{\mathbf{w}}}(t) =& diag\{e^{-j2\pi f_c T_d l}\} \\ &.\mathbf{Q} diag\{\frac{\mu\lambda_l}{1+\mu\lambda_l}(1-e^{-(1+\mu\lambda_l)\alpha t}\}\mathbf{Q}^{-1}\mathbf{h}\end{aligned} \tag{12}$$

and the $P_{RI}(t)$ is calculated by

$$P_{RI}(t) = \frac{1}{2}\epsilon^2 + \frac{1}{2}\mathbf{h}^H\mathbf{Q} diag\{\frac{\lambda_l}{(1+\mu\lambda_l)^2}\}\mathbf{Q}^{-1}\mathbf{h} \tag{13}$$

where ϵ is the error between the real SI $Z(t)$ and the modeled one; $\mathbf{h}$ is the one-column matrix of the modelled tap coefficients $\mathbf{h} = [h_0\ h_1\ ...\ h_{L-1}]^T$; $\mathbf{Q}$ and λ_l are the orthonormal modal matrix and the eigenvalues of the normalized autocorrelation matrix Φ with each element defined by

$$\bar{\Phi}_{XX}(\tau) = \frac{1}{K_1 K_2 T}\int_0^T \Phi_{XX}(t,\tau)dt. \tag{14}$$

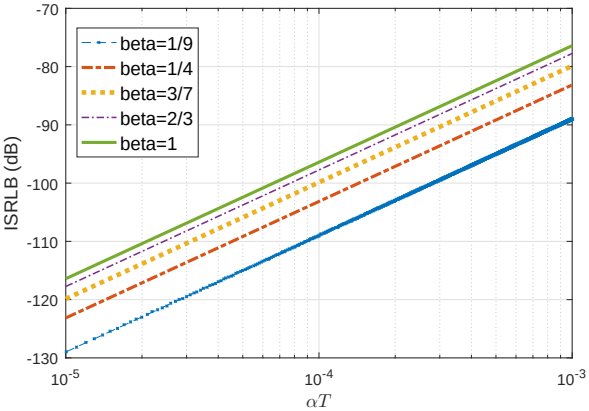

Fig. 4. ISRLB versus αT with various windowing roll-off factors.

It is shown in [4] that the ISR can be calculated from $P_{RI}(t)$ and $P_I(t)$ as

$$ISR = \frac{\epsilon^2 + \mathbf{h}^H\mathbf{Q} diag\{\frac{\lambda_l}{(1+\mu\lambda_l)^2}\}\mathbf{Q}^{-1}\mathbf{h}}{\epsilon^2 + \mathbf{h}^H\Phi\mathbf{h}} \tag{15}$$

Using these formulas, we can determine the weight error functions, the normalized residual interference power, and ISR.

IV. Simulation Results

Simulation is performed with an OFDM system specified in IEEE802.11 standard. Transmitted data is generated with sampling period of $T_s = 5nS$ and modulated using BPSK before going through a 64-point IFFT block. Cyclic prefix is then added which occupies one fourth of an OFDM symbol. IEEE 802.11 windowing function and RC pulse shaping function are utilized with roll-off factors of $\beta = 0.25$. The power of the transmitted signal is set at 0 dBm, and the multiplier dimensional constants are set to be $K_1K_2 = 0.001V^2$ so that $A = 10$. Another loop gain parameter μ is selected as $\mu = 10$. α is determined using the expression of $ISRLB = 10^{-10}$. Simulations are conducted under two scenarios of interference channel which are set as the same as in [4]. Specifically, the first scenario assumes that the reflected paths of interference channel have the delays of multiple T_s so that the interference channel is chosen as $h(t) = 10^{\frac{-25}{20}}\{[\frac{\sqrt{2}}{2} - 0.5j]\delta(t) - 0.4\delta(t - T_s) + 0.4\delta(t - 3T_s)\}$. The second scenario considers the general case of interference channel in which the reflected paths have arbitrary delays, i.e., $h(t) = 10^{\frac{-25}{20}}\{[\frac{\sqrt{2}}{2} - 0.5j]\delta(t) - 0.4\delta(t - 0.9T_s) + 0.4\delta(t - 3.3T_s)\}$. We also investigate the performance of ALMS loop filter with 8 taps spaced at T_s and 16 taps spaced at $T_s/2$.

The convergence curves of the first tap coefficients $\bar{w}_0(t)$ under the first scenario with T_s spaced is presented in Fig.5. At macro scale, the simulated weights coefficients converge to almost the same values calculated from (12). At micro scale shown in the inset, the simulated $\bar{w}_0(t)$ varies with

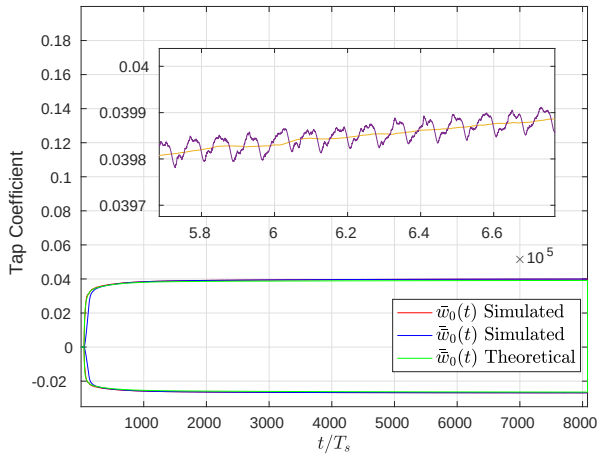

Fig. 5. Weighting coefficients of ALMS loop with T_s and $T_s/2$ spacing: simulated and theoretical results.

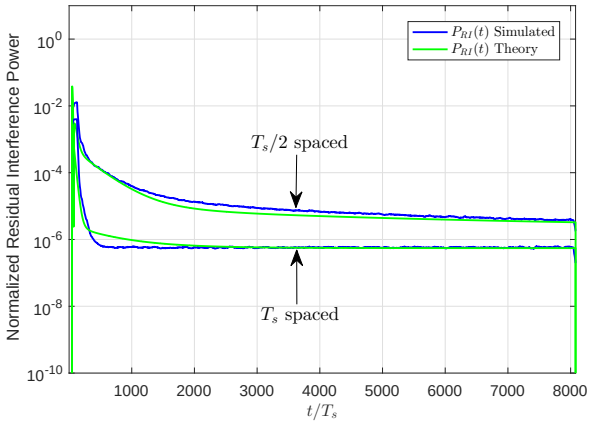

Fig. 6. Simulated and theoretical convergence curves for residual interference power of the ALMS loop with T_s and $T_s/2$ spacing in the first scenario.

period of OFDM symbol T. This figure shows both cyclostationary effect and the expectation in stationary analysis for the weighting error function. The convergence curves of the residual interference power for two cases of tap spacing in the first interference channel scenario are presented in Fig.6. We can see that the simulated curves in both cases coincide with those calculated from (13). The self-interference is canceled at higher level when Ts spacing was utilized. The reason is that modelling error for T_s spacing was zero whereas it is 7.508×10^{-11} for the $T_s/2$ case.

To compare the performance of the ALMS loop in an OFDM system with that in a single carrier one, we use ISR as the performance measure. From (15), ISR can be calculated for different scenarios. The results for both scenarios with different tap delays are presented in Table I. We can see that with the same loop gain, the ALMS filter in OFDM systems can provide a much higher level of suppression to SI. More

TABLE I
ISR OF THE ALMS LOOP

ISR(dB)	Scenario 1		Scenario 2	
	T_s spaced	$\frac{T_s}{2}$ spaced	T_s spaced	$\frac{T_s}{2}$ spaced
Single Carrier	-59.58	-49.17	-17.58	-49.52
OFDM	-76.17	-62.99	-50.85	-59.338

importantly, in case of T_s spaced under the scenario 2, ISR given by ALMS loop in the OFDM system is up to -50.85 dB which is almost three times higher (in dB) than that in the single carrier system. It means that the performance of the ALMS loop in a multi-carrier system is less sensitive to its tap delay spacing. The reason is that the OFDM signal has a superior auto-correlation function such that the modelling error is very small. Specifically, under the general interference channel scenario, the modelling errors (ϵ) of the ALMS loop in OFDM system and single carrier one are 2.0397×10^{-6} and 0.005 respectively.

V. Conclusion

Cyclostationary analysis shows that the performance of the ALMS loop for OFDM system depends on the windowing function used. The loop gain and LPF parameter determine the convergence speed and level of cancellation. Simulation results confirm the theoretical analysis and prove that the ALMS loop in OFDM system has much smaller modelling error and achieve a better level of interference cancellation.

References

[1] Cisco, "White paper: Cisco VNI Forecast and Methodology, 2015-2020 - Cisco," 2016.

[2] A. Sabharwal, P. Schniter, D. Guo, D. W. Bliss, S. Rangarajan, and R. Wichman, "In-band full-duplex wireless: Challenges and opportunities," *IEEE Journal on Selected Areas in Communications*, vol. 32, no. 9, pp. 1637–1652, 2014.

[3] D. Bharadia, E. McMilin, and S. Katti, "Full duplex radios," *Proceedings of the ACM SIGCOMM 2013*, vol. 43, no. 4, pp. 375–386, 2013.

[4] X. Huang and J. Guo, "Radio frequency self-interference cancellation with analog least mean square loop," *to appear in IEEE Transactions on Microwave Theory and Techniques*.

[5] K. E. Kolodziej, J. G. McMichael, and B. T. Perry, "Multitap RF canceller for in-band full-duplex wireless communications," *IEEE Transactions on Wireless Communications*, vol. 15, no. 6, pp. 4321–4334, June 2016.

[6] J. Choi, M. Jain, and K. Srinivasan, "Achieving single channel, full duplex wireless communication," in *MobiCom*. ACM, 2010.

[7] B. Debaillie, D. J. Van Den Broek, C. Lavín, B. Van Liempd, E. A. M. Klumperink, C. Palacios, J. Craninckx, B. Nauta, and A. Pärssinen, "Analog/RF solutions enabling compact full-duplex radios," *IEEE Journal on Selected Areas in Communications*, vol. 32, no. 9, pp. 1662–1673, 2014.

[8] J. Kim, M. S. Sim, M. Chung, D. K. Kim, and C.-B. Chae, "Full-duplex Radios in 5G: Fundamentals, Design and Prototyping," in *Signal Processing for 5G*. Chichester, UK: John Wiley & Sons, Ltd, Aug 2016, pp. 539–560.

[9] Seunghyeon Kim, Youngil Jeon, G. Noh, Youn-Ok Park, Ilgyu Kim, and Hyunchol Shin, "A 2.59-GHz RF self-interference cancellation circuit with wide dynamic range for in-band full-duplex radio," in *IEEE MTT-S International Microwave Symposium (IMS)*, 22–27 May 2016.

[10] T. Huusari, Y. S. Choi, P. Liikkanen, D. Korpi, S. Talwar, and M. Valkama, "Wideband self-adaptive RF cancellation circuit for full-duplex radio: Operating principle and measurements," in *IEEE 81st Vehicular Technology Conference (VTC Spring)*, May 2015.